Low-temperature growth and direct transfer of graphene–graphitic carbon films on flexible plastic substrates

Yong-Jin Kim[1,6]**, Sang Jin Kim**[2,6]**, Myung Hee Jung**[3]**, Kwang Yeol Choi**[3]**,
Sukang Bae**[1,2]**, Seoung-Ki Lee**[2,4]**, Youngbin Lee**[2,4]**, Dolly Shin**[1]**,
Bora Lee**[5]**, Huiyoun Shin**[3]**, Myungshin Choi**[3]**, Kyuho Park**[3]**,
Jong-Hyun Ahn**[2,4] **and Byung Hee Hong**[1,2]

[1] Department of Chemistry, College of Natural Sciences, Seoul National University, Seoul 151-747, Korea
[2] SKKU Advanced Institute of Nanotechnology (SAINT) and Center for Human Interface Nano Technology (HINT), Sungkyunkwan University, Suwon 440-746, Korea
[3] Materials and Components Laboratory, LG Electronics Advanced Research Institute, 16 Woomyeon-Dong, Seocho-Gu, Seoul 137-724, Korea
[4] School of Advanced Materials Science and Engineering, Sungkyunkwan University, Suwon 440-746, Korea
[5] Department of Chemistry, Sungkyunkwan University, Suwon 440-746, Korea

E-mail: byunghee@snu.ac.kr and ahnj@skku.edu

Abstract

We demonstrate low-temperature growth and direct transfer of graphene–graphitic carbon films (G–GC) onto plastic substrates without the use of supporting materials. In this approach, G–GC films were synthesized on copper layers by using inductively coupled plasma enhanced chemical vapor deposition, enabling the growth of few-layer graphene (G) on top of Cu and the additional growth of graphitic carbon (GC) films above the graphene layer at temperatures as low as 300 °C. The patterned G–GC films are not easily damaged or detached from the polymer substrates during the wet etching and transfer process because of the van der Waals forces and π–π interactions between the films and the substrates. Raman spectroscopy reveals the two-dimensional hexagonal lattice of carbon atoms and the crystallinity of the G–GC films. The optical transparency and sheet resistance of the G–GC films are controlled by modulating the film thickness. Strain sensors are successfully fabricated on plastic substrates, and their resistance modulation at different strains is investigated.

S Online supplementary data available from stacks.iop.org/Nano/23/344017/mmedia

(Some figures may appear in colour only in the online journal)

1. Introduction

The preparation of graphene films on plastic substrates has attracted much attention for fabrication of emerging devices for transparent, flexible, foldable, or wearable platforms due to its high flexibility, conductivity, and transparency [1–8].

Recently, tremendous progress in graphene growth and transfer methods has enabled the fabrication of large-scale graphene films on flexible plastic substrates [1–3, 5]. However, a difficulty in dealing with two-dimensional carbon sheets of one atomic thickness often results in mechanical damage or deformation (e.g., tearing, fracture, folding, corrugation, wrinkling, etc) on the surface of the graphene. Additionally, the supporting polymer materials required

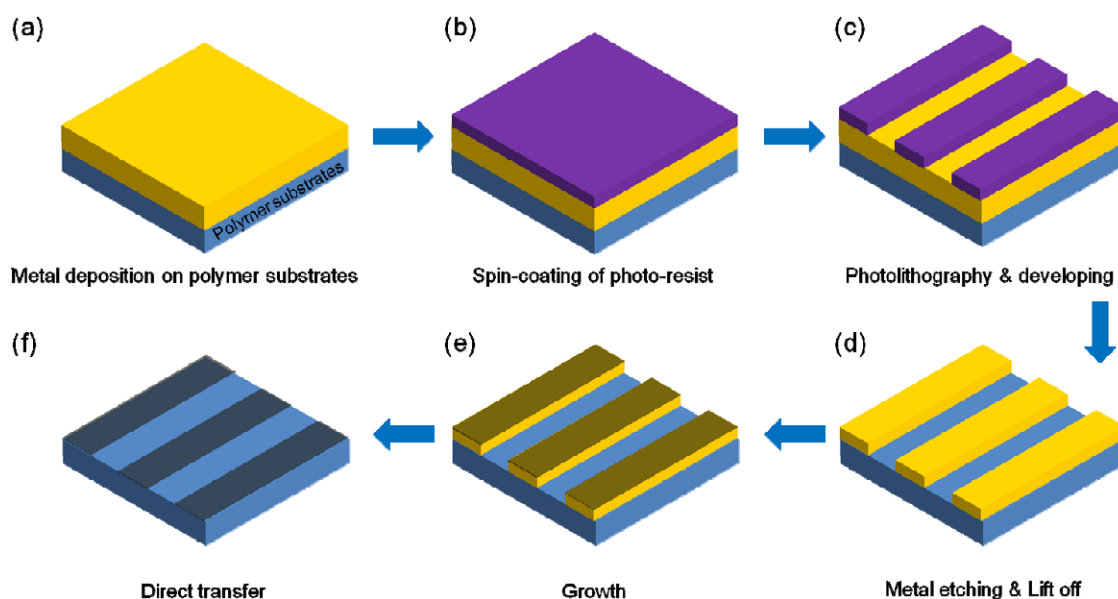[6] These authors contributed equally to this work.

Figure 1. Schematic diagram of the process used to fabricate G–GC films on plastic substrates. (a) Deposition of metal films on the plastic substrates by sputtering. (b) Spin-coating of photoresist films on the substrates. (c) Formation of an etching mask by conventional lithography. (d) Chemical etching of the metal films and lift-off of the photoresist. (e) Growth of a regular array of G–GC films on the metal/plastic substrates using plasma enhanced chemical vapor deposition. (f) Wet etching of the metal layers and direct transfer of the G–GC films onto the plastic substrates.

for the transfer process may contaminate the surface of the graphene [5, 9–11]. These problems associated with the etching and transferring method may be solved by direct growth of the G–GC films on the plastic substrates. Nevertheless, the high growth temperature of the chemical vapor deposition method precludes the use of flexible plastic substrates, which have low melting temperatures [1–3, 5]. Furthermore, the low solubility of carbon atoms into the metal catalysts makes it difficult to grow graphene films at temperatures below the melting point of the plastic. These obstacles can be circumvented by plasma enhanced chemical vapor deposition, which enables the decomposition of the hydrocarbons and increases the solubility of carbon at low temperature [12–14]. Additionally, the van der Waals forces and π–π interactions between the G–GC films and the substrates allow direct transfer of the films to the plastic substrates without the use of supporting materials. Here, we report on the low-temperature growth and direct transfer of G–GC films onto flexible plastic substrates using plasma enhanced chemical vapor deposition.

2. Experimental details

2.1. Synthesis of graphene–graphitic carbon (G–GC) films on plastic substrates

Our approach for low-temperature growth of G–GC films on plastic substrates is schematically shown in figure 1. G–GC films were synthesized on metal thin films deposited on the plastic substrates using inductively coupled plasma enhanced chemical vapor deposition (ICP-CVD). First, 300 nm thick copper (Cu) films were deposited on polyimide (PI) substrates

using a radio frequency (RF) sputtering system. After spin-coating photoresists on the metal-coated PI substrates, regular line patterns were fabricated using photolithography. Subsequently, metal line arrays were defined by wet chemical etching of Cu layers by exposing them to the etchant solution. Finally, the photoresist mask layers on the substrates were removed by immersing them in acetone. For the synthesis of G–GC films on plastic substrates, the ICP-CVD system was adopted to decompose the hydrocarbon and increase the solubility of the carbon atoms at low temperature. First, an as-prepared plastic substrate was inserted into an ICP-CVD chamber and heated to 300 °C. After reaching 300 °C, the surface oxide layer on the metal catalyst was removed by plasma treatment with H_2 flow at 30 standard cubic centimeters per minute (sccm) at 20 mTorr. Graphene films were selectively grown on the metal patterns for 3 min under a mixture of C_2H_2 and Ar gases with flow rates of 3 and 60 sccm, respectively. During the growth, the reactor pressure was maintained at 5 mTorr. The sample was cooled rapidly to room temperature under flowing Ar at a pressure of 5 mTorr. After the growth, the patterned G–GC films were directly transferred onto the plastic substrates by removing the metal catalyst underneath the films. After the metal thin films had been etched away by an aqueous iron (III) chloride ($FeCl_3$) solution, the patterned films were detached from the metal layers and adhered to the plastic substrates.

2.2. Characterization of the G–GC films on plastic substrates

The process of wet chemical etching and direct transfer of the G–GC films was observed using optical microscopy (OM; wm0039000a, Microscopes). The structural quality
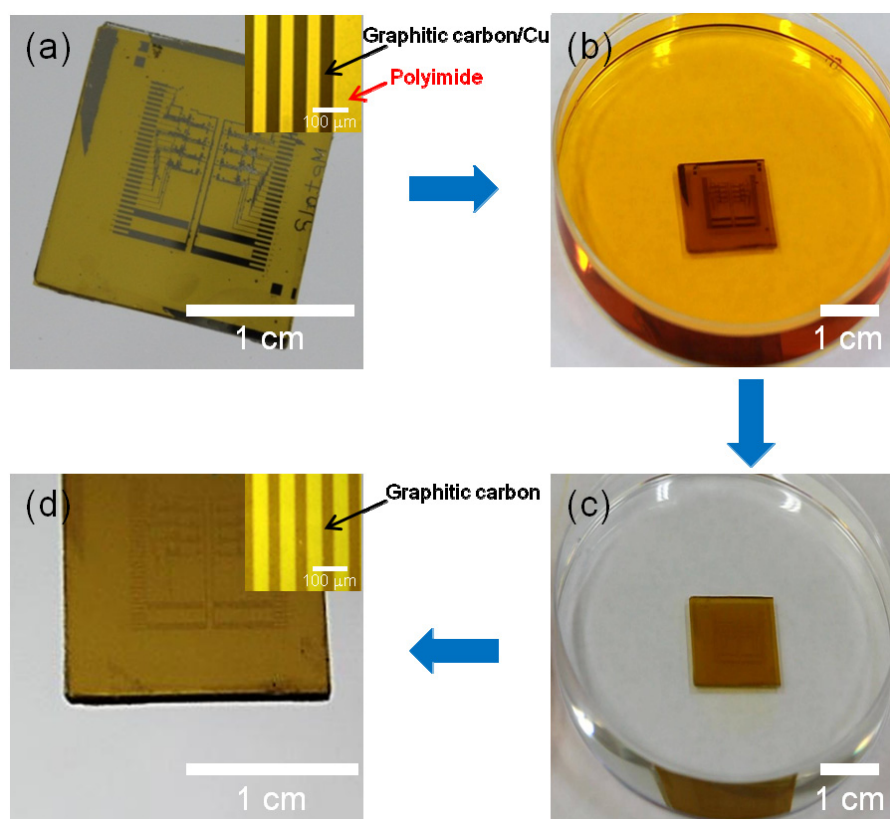
Figure 2. Photographs of the process used for etching and transferring of G–GC films onto plastic substrates. (a) As-synthesized G–GC films on Cu/PI substrates. The inset image displays a large array of patterned G–GC films formed on the PI substrates. (b) Wet chemical etching of the underlying Cu layers by FeCl$_3$ solution. (c) Washing and cleaning with deionized water. The patterned films were not easily damaged or detached from the plastic substrates during the chemical etching and rinsing. (d) A transferred G–GC film on a PI substrate. The inset image shows that the transferred samples on the plastic substrates exhibit clear contrast between the G–GC and the substrates.

and crystallinity of the G–GC films were inspected using high-resolution transmission electron microscopy (TEM) (Titan G2 60–300, FEI Company). For the cross-sectional and high-resolution TEM imaging, the samples were milled with 30 kV accelerated Ga ions using a focused ion beam machine (Helios NanoLab 450, FEI Company). The structural properties of the G–GC films were further investigated by Raman spectroscopy (RM 1000-Invia, Renishaw). Raman spectra were recorded by using an argon ion laser (514 nm) as the excitation source with a notch filter of 50 cm^{-1}. The typical scan range was from 1000 to 3000 cm^{-1} and the instrumental resolution was 1.0 cm^{-1}. The optical transmittance of the films was measured using an ultraviolet–visible spectrometer (UV-3600, Shimadzu) after wet chemical etching and transferring the G–GC films to the plastic substrates. The sheet resistances of the films were measured by the van der Pauw four-probe method using a Hall measurement system [15]. G–GC films with an average width of 200 μm and length of 180 mm were used for strain sensor device applications. Indium electrodes were attached to both ends of the samples to minimize contact resistance. To evaluate the effect of mechanical deformation on the resistance of the films, the samples were loaded onto a holding stage and stretched to a tensile strain of 0.1%. The strain was maintained for 20 s, and then the resistance of the G–GC films was recorded. The resistances of the

samples were recorded continuously until the applied strain reached 1%.

3. Results and discussion

Figures 2(a)–(d) are representative photographs of the direct transfer process of patterned G–GC films on polymer substrates. As shown in figure 2(a), the OM image clearly illustrates a large array of patterned films formed on the PI substrates after the growth. As we will discuss later, the formation of G–GC films on the metal catalysts was studied using micro-Raman spectroscopy after transferring them onto the SiO$_2$/Si substrates. Without the use of supporting polymer materials such as poly(methyl methacrylate) (PMMA), poly(dimethylsiloxane) (PDMS), or thermal release tape, the G–GC film/metal/PI substrate was soaked in Fe$_3$Cl solution to remove the metal layers (figure 2(b)). We found that the thickness of the metal films is critical in the chemical etching of metal and the direct transfer process. After growth, Cu thin films with a thickness of less than 300 nm were not completely etched due to the strong adhesion between the Cu films and the polymer substrates. In contrast, when 300 nm thick Cu layers were used, the G–GC films were easily separated from the Cu thin films and transferred onto the polymer substrates. The difference in chemical etching depending on the metal thickness may result from the de-wetting of the Cu thin

films from the polymer substrates and the penetration of the etchant solution into the gap between the metal layer and the substrate. After the metal layers were etched, the separated G–GC films adhered to the polymer substrates by the van der Waals forces acting between them. Usually, without polymer support coating, graphene films grown on Cu foils are easily torn or broken into pieces during the chemical etching and transferring process [1–3]. In contrast, the patterned G–GC films were not easily damaged or detached from the plastic substrates during the chemical etching and rinsing as shown in figure 2(c). The strong adhesion of the G–GC films to the substrates may originate from the π–π interactions between the delocalized electrons of the graphene and the aromatic rings of the polyimide. As previously reported, the binding energy of aromatic molecules to graphene has been calculated to be 40–90 meV/C-atom depending on the chemical structure of the aromatic molecules [16]. Even though the PI plastic includes disordered aromatic molecules, the local interaction between the graphene and the ordered aromatic molecules is strong enough for transfer of the graphene films without the use of polymer support layers. A high-magnification optical image of G–GC films on the polymer substrates is shown in figure 2(d) and exhibits a clear difference in the contrast between the films and the substrates. This direct transfer method without the use of polymer supporting materials makes it possible to produce a clean graphene film surface without any residues that often originate from the polymer supports.

High-resolution TEM and Raman spectroscopy were employed to evaluate the structural quality of the G–GC films grown by ICP-CVD method. As shown in figure 3(a), a high-resolution TEM image measured along the cross-sectional direction of the G–GC film displays a highly ordered lattice image only on the surface of the Cu film, indicating the formation of a crystalline graphene film. The thickness of the crystalline graphene ranged from 3 to 4 nm, corresponding to approximately 8–10 layers of graphene. On the surface of the few-layer graphene, however, amorphous carbon films or G–GC layers were simultaneously formed. Since the crystal nucleation and growth of carbon on few-layer graphene are totally different from the growth of graphene films on Cu films, the deposition of carbon films occurred on the surface of the few-layer graphene. Note that it might be possible to grow only few-layer graphene on Cu substrates to reduce the quantity of carbon source or growth time, which prevents the deposition of amorphous or G–GC layers.

Figure 3(b) shows the Raman spectrum of the G–GC films grown on Cu layers and transferred onto SiO_2/Si substrates. The Raman spectrum showed a dominant peak at 1610 cm^{-1} (G-band) and a weak peak at 2650 cm^{-1} (2D-band), indicating that the synthesized G–GC films maintained the sp^2 bonded hexagonal lattice structure [17]. The strong peak observed at 1330 cm^{-1} (D-band) corresponds to the breathing mode of the hexagonal aromatic rings and is tentatively attributed to the existence of defects, local disorder, or sp^3 bonds in the G–GC films [17, 18]. As reported previously, an intense and narrow G-band, a weak D-band, and a very intense 2D-band are the typical features
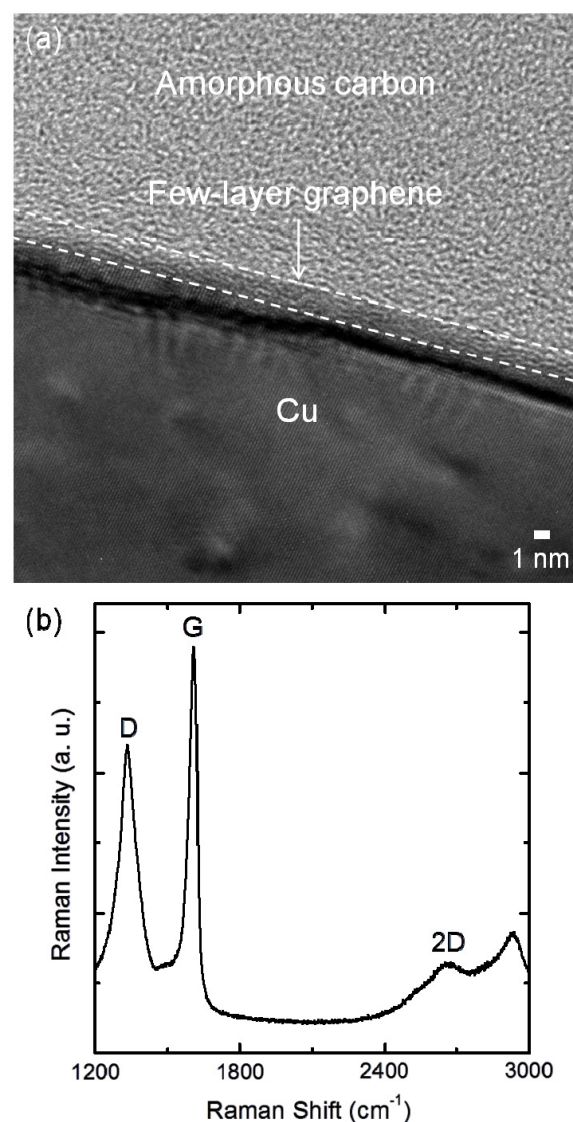

Figure 3. Structure characteristics of G–GC films grown on plastic substrates. (a) Transmission electron microscopy images of G–GC films on Cu/PI substrates. (b) Raman spectrum of the G–GC films transferred to the SiO_2/Si substrates.

of continuous single- or few-layer graphene. The shape of the 2D-band and the ratio of its intensity relative to that of the G-band are strongly dependent on the number of layers [1–3]. Nevertheless, these characteristics are not observed from our G–GC films. Instead, an I_D/I_G ratio of 0.8 and a narrow G-band with a full width at half maximum (FWHM) value of 40 cm^{-1} are observed, indicating that the G–GC films are composed of the microcrystalline graphite inclusions and amorphous carbon matrix [18]. This result is consistent with the TEM observation of the coexistence of amorphous carbon films or G–GC layers on the surface of few-layer graphene. In addition, a peak shift of the G-band from 1580 to 1610 cm^{-1} is clearly observed, indicating that G–GC films with small crystallite sizes or abundant edges are formed. This observation strongly suggests that the formation of few-layer graphene with small grain size is due to the enhanced nucleation and reduced grain growth on the surface of metal layers at low growth temperatures [19–22].
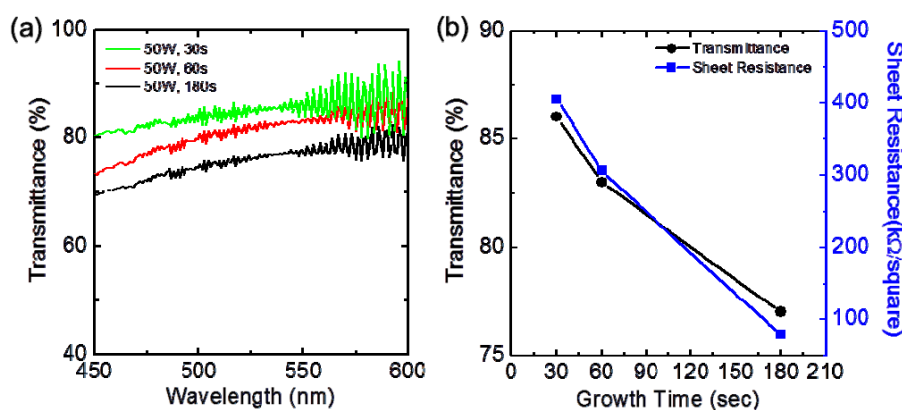
Figure 4. Optical and electrical characteristics of the G–GC films on the plastic substrates. (a) Transmittance curves of the G–GC films with different growth times of 30, 60, and 180 s. (b) Transmittance and sheet resistance of the G–GC samples as a function of the growth time.

An ultraviolet–visible spectrometer was used to investigate the optical transparency of the G–GC films on the polymer substrates after the wet etching of the metal layer and direct transfer of the samples onto the polymer substrates. Figure 4(a) displays the transmittances of G–GC films for various growth times of 30, 60, and 180 s with fixed growth conditions. In the visible wavelength ranging from 450 to 600 nm, the transmittance of the films systematically decreases with increasing growth time. The decrease in the transmittance values may originate from the increased thickness of the G–GC films with respect to the growth time, resulting in the increased light absorption (see supporting information, figure S1 available at stacks.iop.org/Nano/23/344017/mmedia). As shown in figure 4(b), the transmittances (at 550 nm wavelength) of G–GC films grown for 30, 60, and 180 s are found to be 86%, 83%, and 77%, respectively. These transmittance values of G–GC films on polymer substrates are comparable to those of chemically exfoliated and CVD graphene films [20–25]. We further investigated the dependence of the transmittance on the plasma power with other growth condition fixed (supporting information, figure S2 available at stacks.iop.org/Nano/23/344017/mmedia). The transmittance of the G–GC films increases from 64% to 77% when the applied plasma power is reduced from 200 to 50 W. This may be responsible for the decrease in the film thickness (figure S1 available at stacks.iop.org/Nano/23/344017/mmedia). This result clearly indicates that the optical transparency of G–GC films is easily controlled by varying the film thickness, which can be readily determined by changing growth conditions such as duration, growth temperature, and plasma power.

Figure 4(b) depicts the sheet resistance of the G–GC films as a function of the growth time. As the growth time increases, the sheet resistance of the G–GC films is reduced. The reduced sheet resistance, in turn, may be resulting from the increase in the film thickness. The sheet resistances of the three G–GC films grown for different durations of 30, 60, and 180 s are 400, 300, and 80 kΩ per square, respectively. The sheet resistance value of G–GC films on plastic substrates is comparable to that of graphene directly grown on glass or quartz substrates (a typical sheet resistance value in the range

of 2.5–40 kΩ per square) [20]. However, this sheet resistance of the G–GC films is two or three orders of magnitude larger than that of CVD graphene films (a typical sheet resistance value in the range of 10–100 Ω per square) [1–3, 5]. The discrepancy in the electrical properties of G–GC films and continuous graphene films may result from the differences in their crystallinity, structural defects, and thickness. It should be noted that the sheet resistances of G–GC films cannot be directly compared to those of graphene films because the sheet resistance is a function of the thickness of the film.

The modulation of the resistance of G–GC films was investigated under uniaxial tensile strain ranging from 0% to 1% (figure 5). The upper inset image in figure 5(a) shows the strain sensor device after applying the strain. Figures 5(a) and (b) display the change of resistance of the G–GC films as a function of time and applied strain. Immediately after applying the tensile stress, the resistance rapidly increased and then stabilized for 20 s. The resistance of the G–GC films exhibited a gradual increase up to a tensile strain of 0.8% (measured at 340 s). In particular, it increased linearly from 31.64 to 31.69 MΩ with applied strains of 0.1% and 0.8% (figure 5(b)). The resistance at strains lower than 0.1% shows just a slight change due to the flattening of wrinkles which occur during the growth and etching process. The strong dependence of the resistance of the G–GC films on the structural deformation may originate from changes in the electronic band structure or the creation of charge carrier scattering centers. However, further stretching of the sample over 0.8% did not show any increase of resistance with respect to the applied tensile stress. This could be due to mechanical failure in applying the tensile stress to the G–GC films.

4. Conclusion

In summary, we have developed a low-temperature growth method for G–GC films using inductively coupled plasma enhanced chemical vapor deposition. A direct transfer method was used to transfer the G–GC films onto plastic substrates without the use of supporting materials. Owing to the van der Waals forces and π–π interactions between the films and the plastic substrates, the patterned G–GC films were
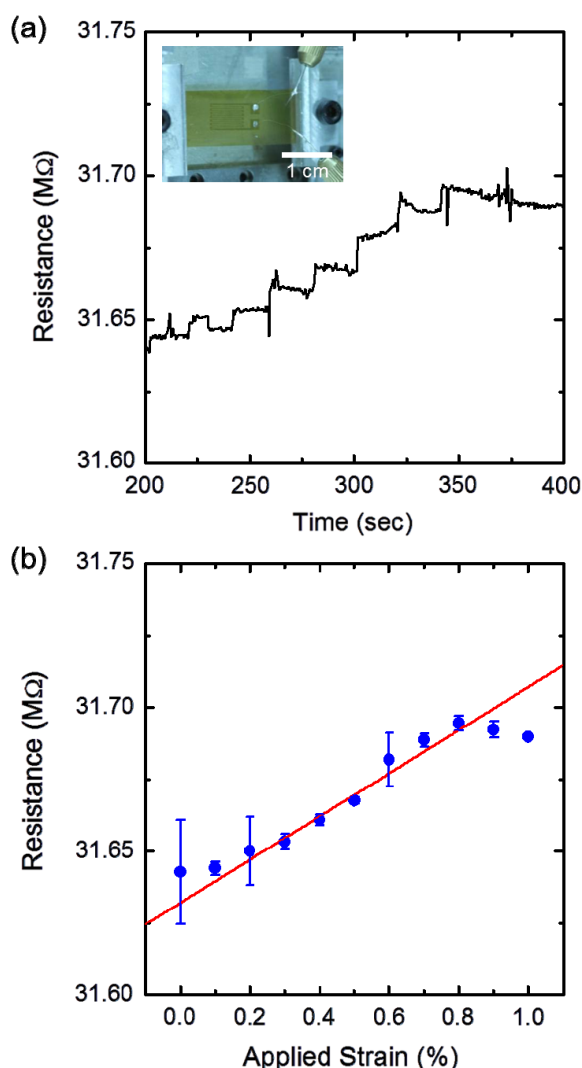
Figure 5. Modulation of the resistance of the G–GC films under tensile strain. (a) Change of the resistance of the G–GC films as a function of time. The inset is a photographic image of the strain sensor device after applying the strain. (b) The resistance response of the films under different strains. The resistance increases linearly from 31.64 to 31.69 MΩ with applied strains of 0.1% and 0.8%. All scale bars represent 1 cm.

not damaged or detached from the substrates during the transferring process. The electrical and optical properties of the G–GC samples could be modulated by varying the growth time, growth temperature, and plasma power. Strain sensors based on G–GC films were successfully fabricated on plastic substrates, and their resistance modulation with different strains was investigated. More generally, this low-temperature growth and direct transfer method could provide a general and rational route for the synthesis of graphene films on flexible and stretchable plastic substrates for various device applications [26–31].

Acknowledgments

References

[1] Reina A, Jia X T, Ho J, Nezich D, Son H B, Bulovic V, Dresselhaus M S and Kong J 2009 *Nano Lett.* **9** 30
[2] Kim K S, Zhao Y, Jang H, Lee S Y, Kim J M, Kim K S, Ahn J H, Kim P, Choi J Y and Hong B H 2009 *Nature* **457** 706
[3] Li X S *et al* 2009 *Science* **324** 1312
[4] De Arco L G, Zhang Y, Schlenker C W, Ryu K, Thompson M E and Zhou C W 2010 *ACS Nano* **4** 2865
[5] Bae S *et al* 2010 *Nature Nanotechnol.* **5** 574
[6] Kim B J, Jang H, Lee S K, Hong B H, Ahn J H and Cho J H 2010 *Nano Lett.* **10** 3464
[7] Lee C-H, Kim Y-J, Hong Y J, Jeon S R, Bae S, Hong B H and Yi G-C 2011 *Adv. Mater.* **23** 4614
[8] Han T-H, Lee Y, Choi M-R, Woo S-H, Bae S-H, Hong B H, Ahn J-H and Lee T-W 2012 *Nature Photon.* **6** 105
[9] Moser J, Barreiro A and Bachtold A 2007 *Appl. Phys. Lett.* **91** 163513
[10] Lock E H *et al* 2012 *Nano Lett.* **12** 102
[11] Lin Y-C, Lu C-C, Yeh C-H, Jin C, Suenaga K and Chiu P-W 2012 *Nano Lett.* **12** 414
[12] Malesevic A, Vitchev R, Schouteden K, Volodin A, Zhang L, Van Tendeloo G, Vanhulsel A and Van Haesendonck C 2008 *Nanotechnology* **19** 305604
[13] Malesevic A, Kemps R, Vanhulsel A, Chowdhury M P, Volodin A and Van Haesendonck C 2008 *J. Appl. Phys.* **104** 084301
[14] Shang N G, Papakonstantinou P, McMullan M, Chu M, Stamboulis A, Potenza A, Dhesi S S and Marchetto H 2008 *Adv. Funct. Mater.* **18** 3506
[15] van der Pauw L J 1958 *Philips Res. Rep.* **13** 1
[16] Björk J, Hanke F, Palma C-A, Samori P, Cecchini M and Persson M 2010 *J. Phys. Chem. Lett.* **1** 3407
[17] Ferrari A C *et al* 2006 *Phys. Rev. Lett.* **97** 187401
[18] Schwan J, Ulrich S, Batori V, Ehrhardt H and Silva S R P 1996 *J. Appl. Phys.* **80** 440
[19] Rummeli M H, Bachmatiuk A, Scott A, Borrnert F, Warner J H, Hoffman V, Lin J H, Cuniberti G and Buchner B 2010 *ACS Nano* **4** 4206
[20] Zhang L C, Shi Z W, Wang Y, Yang R, Shi D X and Zhang G Y 2011 *Nano Res.* **4** 315
[21] Lee C M and Choi J 2011 *Appl. Phys. Lett.* **98** 183106
[22] Kim K B, Lee C M and Choi J 2011 *J. Phys. Chem. C* **115** 14488
[23] Li X L, Zhang G Y, Bai X D, Sun X M, Wang X R, Wang E and Dai H J 2008 *Nature Nanotechnol.* **3** 538
[24] Eda G, Fanchini G and Chhowalla M 2008 *Nature Nanotechnol.* **3** 270
[25] Liang Y, Frisch J, Zhi L, Norouzi-Arasi H, Feng X, Rabe J P, Koch N and Mullen K 2009 *Nanotechnology* **20** 434007
[26] Bae S, Kim S J, Shin D, Ahn J-H and Hong B H 2012 *Phys. Scr.* **T146** 014024
[27] Shin D, Bae S, Yan C, Kang J, Ryu J, Ahn J H and Hong B H 2012 *Carbon Lett.* **13** 1
[28] Ihm K, Lim J T, Lee K-J, Kwon J W, Kang T-H, Chung S, Bae S, Kim J H, Hong B H and Yeom G Y 2010 *Appl. Phys. Lett.* **77** 032113
[29] Kim Y-T, Han J H, Hong B H and Kwon Y-U 2010 *Adv. Mater.* **22** 515
[30] Kang J, Kim H, Kim K S, Lee S-K, Bae S, Ahn J-H, Kim Y-J, Choi J-B and Hong B H 2011 *Nano Lett.* **11** 5154
[31] Huh S, Park J, Kim K S, Hong B H and Kim S B 2011 *ACS Nano* **5** 9799

6